

Analysis and Testing of a LIDAR-Based Approach to Terrain Relative Navigation for Precise Lunar Landing

Andrew E. Johnson¹ and Tonislav I. Ivanov²

Jet Propulsion Laboratory, California Institute of Technology, 4800 Oak Grove Drive, Pasadena, CA, 91109

Capability for precise lunar landing is the goal for future NASA missions. A LIDAR-based terrain relative navigation (TRN) approach lets us achieve this goal and also land under any illumination conditions. Results from field test data showed that the LIDAR TRN algorithm obtained position estimates with mean error of about 20 meters and standard deviations of about 10 meters. Moreover, the algorithm was capable of providing 99% correct estimates by assessing the local terrain relief in the data. Also, the algorithm was able to handle initial position uncertainty of up to 1.6 km without performance degradation.

Nomenclature

ALHAT	=	Autonomous Landing and Hazard Avoidance Technology
LIDAR	=	Light Detection And Ranging
TRN	=	terrain relative navigation
DEM	=	digital elevation map
NTS	=	Nevada Test Site
DV	=	Death Valley
USGS	=	United States Geological Survey
UTM	=	Universal Transverse Mercator
ECEF	=	Earth Centered Earth Fixed Frame
μ	=	Valid Mean Error
σ	=	Valid Standard Deviation of Error
V/S	=	Valid Over Sure Fraction
V/T	=	Valid Over Total Fraction
P2V	=	Peak-to-Valley
TRI	=	Terrain Relief Index

I. Introduction

PRECISE landing on the surface of the Moon is the goal for future lunar missions of NASA. Such capability will enable scientists to get closer to a point of interest and to access rougher terrain. However, traditional lunar landing approaches, based on inertial sensing, do not have the navigational precision to meet this goal. To address this shortcoming, several terrain relative navigation (TRN) approaches have been proposed.¹⁻⁶ These approaches sense the terrain during descent and augment the inertial navigation by providing, in real-time, position or bearing estimates relative to known surface landmarks. From these estimates, the navigational precision can be increased to a level that meets a requirement of landing within 90 m of a predetermined location.⁷

The Autonomous Landing and Hazard Avoidance Technology (ALHAT) project of NASA is developing LIDAR-based terrain relative navigation algorithm.⁸⁻¹⁰ Unlike others, this is an active range sensing approach that can operate under any illumination conditions in order to achieve landing anywhere on the Moon at any time of day. The proposed TRN approach is intended for use during the braking burn phase of a lander, after it de-orbits. During this phase, the lander travels a significant distance downrange at a shallow path angle; thus, the cumulative LIDAR data forms a long contour. Additionally, the LIDAR can be placed on a single-axis gimbal that swings in the cross-track direction to produce a wider contour. After collection, the LIDAR data is projected into a digital elevation map (DEM) using the most current position estimate for the lander. To obtain a position correction, this “LIDAR DEM”

¹ Principal Member of Technical Staff, Optical Navigation Group, MS 301-121, AIAA member

² Associate Member of Technical Staff, Computer Vision Group, MS 198-236

is correlated with a “reference DEM” constructed from a-priori reconnaissance, such as the Lunar Reconnaissance Orbiter data. High-fidelity simulation of the LIDAR TRN has shown that both regular and wide contours can achieve the ALHAT 90 m precision objective.¹

This paper describes the performance of the LIDAR-based TRN approach on data collected during a recent field test described in section II. More detail on the algorithm is given in section III. The approach produces position estimates and confidence using internal metrics introduced in section IV. In most field test flights, as shown in section V, the confident estimates have error typically less than 50 m. Misalignments are the likely causes of the large position errors in other flights. After optimizing the confidence threshold in four test flights, 99% of the confident estimates had error less than 90 m. In addition, in Section VI, studies were conducted to assess the sensitivity to confidence metric, contour length, map resolution, and initial position uncertainty.

II. Field Test Description

To further mature LIDAR TRN, as well as other TRN approaches, ALHAT conducted a field test in June and July of 2009. For this test, a fixed-wing aircraft was outfitted with a suite of TRN sensors, along with sensors to provide ground truth position and attitude. A gimbaled platform contained the flash LIDAR sensor and different gimbal modes resulted in different contour widths. Details on the field test implementation, platform, and ground truth trajectory generation can be found in [Keim 2010]¹². A total of eight data collection flights were flown. For most flights, the plane flew horizontally at 60 m/s. The flights were conducted at 2, 4, and 8 km altitudes over two test sites: Death Valley (DV) and Nevada Test Site (NTS). A variety of terrain was imaged including mountains, hills, washes, dry lakebeds, and craters. Each flight had between one and two hours of valid data.

NTS and DV were selected as test sites for the field test because of the lack of vegetation over large areas and the variety of terrain relief. NTS in particular was selected because it has a large crater field on a flat terrain, analogous to the lunar mare. DV in particular was selected because of the mountainous regions and associated foothills that are analogous to the lunar uplands.

III. Position Estimation Process

The LIDAR TRN algorithm took as inputs a reference map and a LIDAR map. The reference maps for DV and NTS were obtained by downloading the 1/9 arcsecond National Elevation Datasets from the USGS Seamless server. These maps were represented in the UTM map projection and had nominal resolution of 5 m. The LIDAR maps were constructed out of the field test data. To do this, 3D point clouds were generated from the raw LIDAR data. Then, these point clouds were projected into the UTM coordinate frame to obtain the LIDAR DEMs. In the end, the TRN algorithm was applied to produce the position estimates. These steps are described in more detail below. A result of applying the LIDAR TRN algorithm to a short contour from NTS is shown in Fig. 1. The correlation correctly computed the position shift to align the LIDAR DEM with the reference DEM.

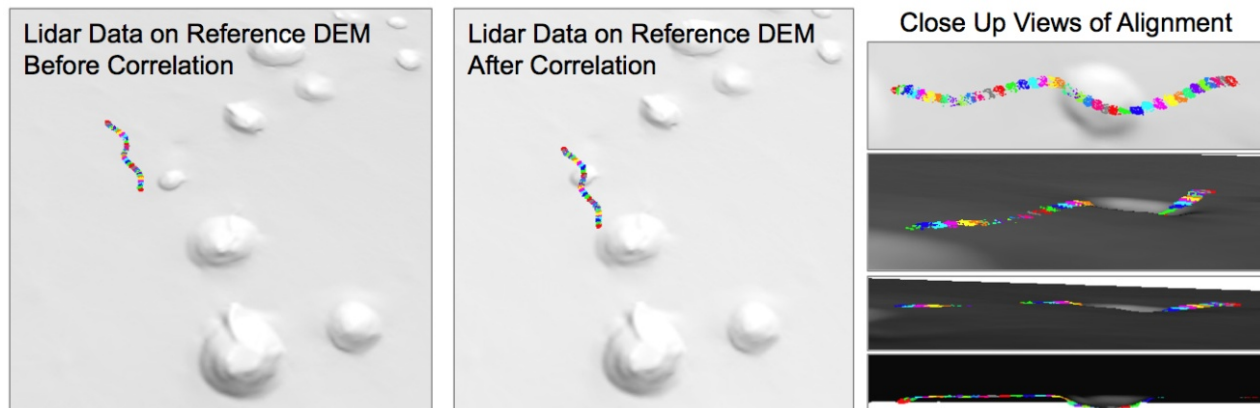


Figure 1. LIDAR TRN result for a short contour over NTS.

A. Generating 3D Point Clouds

The flash LIDAR data consisted of 128 by 128 pixel images. Each pixel in a LIDAR image consisted of 20 timed intensities of the return laser pulse. First of all, pixels that constantly yielded erroneous readings or did not trigger, i.e. did not register a reading, were disregarded. Next, the maximum intensity for each remaining pixel was determined by finding the peak of a 6th order polynomial fit to the timed return pulse intensities. The corresponding time-of-flight for this maximum, as measured by the LIDAR’s clock, was then multiplied by the speed of light to

yield a range for that pixel. Also, the ranges were calibrated to deal with drifting clock rate and pixel-to-pixel non-uniformities. Additionally, to remove any remaining outliers, a local median filter was applied to the ranges. Finally, a 3D point cloud was generated for each image by computing the rays for each pixel using a perfect perspective camera projection.

B. Constructing the LIDAR DEM

The 3D point clouds were represented in the LIDAR sensor coordinate frame. They needed to be transformed into the UTM frame to generate a LIDAR DEM with the same frame as that of the reference map. Beforehand, a flight trajectory was computed that defined the position and attitude of the LIDAR in the Earth Centered Earth Fixed Frame (ECEF). This trajectory was interpolated to construct rigid transformations that, at each LIDAR image instance, mapped the sensor frame to the ECEF. Sequentially, the 3D point cloud for each image was transformed into the ECEF, then into latitude/longitude/height, and finally into the UTM frame. After 3D point clouds from several sequential LIDAR images were transformed into the UTM frame, the new points were projected into a grid using bilinear interpolation to form the LIDAR DEM contour. The LIDAR DEM resolution was set to 5 m to match the one of the reference DEM. The width of the LIDAR contour depended on whether the gimbal was moving or not during flight. The length of the contour depended on the number of images used to form it and was adjusted to tune the performance.

C. Apply LIDAR TRN Algorithm

The bounds of the LIDAR DEM, increased by the position uncertainty of 200 m, were used to crop the large reference DEM. The LIDAR DEM and the cropped reference DEMs were matched using a floating-point correlation algorithm that handled missing data. The maximum value in the correlation map resulting from the algorithm corresponded to the horizontal shift between the contour and the reference DEM. To increase the precision of this shift, a bi-quadratic fit was made to a 3 by 3 neighborhood around the correlation peak to compute a sub-pixel maximum. This shift in pixels was converted to a shift in meters using the DEM pixel size. The process described above was automated and all flights were processed at nominal parameters. Additionally, studies were conducted on a smaller subset to determine sensitivity to driving parameters.

IV. Analysis Metrics

A. Performance Metrics

The purpose of TRN was to provide accurate position estimates. The error of an estimate was determined by the difference between the position estimated by the algorithm and the position computed from the ground truth data. Recall that the ALHAT requirement was to land within 90 m horizontal distance of the intended landing point. Thus, for the purpose of this analysis, a “correct” position estimate was defined as one that has a position error less than 90 m and an incorrect estimate was one that had a position error greater than 90 m.

In addition to estimating position, the TRN algorithm was expected to establish a level of confidence for the estimates. As described below, this confidence was established by applying thresholds on one of more metrics internal to the algorithm in such a way that the estimates above the thresholds had high precision. The algorithm would pass on to the navigation filter every estimate in which it was confident. In this study, such estimate was defined as “sure.”

If an estimate was both correct and sure, it was deemed “valid.” The following performance metrics were established:

- Valid Mean Error (μ): the mean horizontal position error of the correct and sure estimates. This metric established the expected accuracy of such estimates.
- Valid Standard Deviation of Error (σ): the standard deviation of the horizontal position error of the correct and sure estimates. This metric described the variation in accuracy of such estimates.
- Valid Over Sure Fraction (V/S): The ratio of the number of correct and sure estimates over the number of all sure estimates. This metric described how often an incorrect estimate would be passed to navigation.

B. Confidence Metrics

These TRN metrics assigned a measure of confidence to the TRN estimates and decided which estimates would be used in navigation. Mostly, the estimates in which TRN was sure were also correct, but sometimes they had an error as large as the original position uncertainty. The aim was to achieve the greatest number of valid estimates while allowing very few incorrect estimates to be passed on to navigation.

The correlation peak height, correlation peak width, and peak ratio were output as correlation metrics. These metrics were computed after the algorithm was run and described properties of the correlation DEM matching procedure done by TRN. Additionally, four terrain metrics were calculated from the LIDAR contour. These metrics were computed before the algorithm was run and describe properties of the terrain contour used in TRN matching. It was supposed that the terrain relief and the geometry of the contour related to the TRN error. All terrain metrics were computed locally, on a sliding 100 m by 100 m window, and then the overall maximum result for the contour was taken.

The TRN confidence metrics were:

- Correlation peak height – the height of the correlation peak as defined by the bi-quadratic fit
- Correlation peak width – the maximum width of the correlation peak
- Peak ratio – the ratio in heights of the correlation peak and the second highest peak
- Peak-to-Valley (P2V) – the difference between the highest and the lowest elevation in the terrain contour after it is projected on the median plane to remove the effect of overall slope
- Terrain Relief Index (TRI) – the expected standard deviation of elevations among neighboring pixels.¹¹
- Contour size – the total number of DEM pixels in the contour
- Contour shape – a measure of length and width of the contour as described by the two eigenvalues of the scatter matrix of the x and y coordinates of the contour points

V. Performance Analysis of Flights

Based on the contour length sensitivity study describe in the next section, 75 consecutive flash LIDAR images were used to construct each contour in every flight. Given the 10 Hz rate of the LIDAR and the 60 m/s speed of the aircraft, this resulted in contour length of 450m. The processing steps, described in Section III, were applied to each contour and the TRN position correction was recorded along with all the confidence metrics mentioned above. Since the ground truth trajectory was used to transform the LIDAR samples into the map frame, the position correction should have been zero; thus, the computed correction was actually the error in position estimation. However, the

Table 1. Comparison of position estimation performance.

		P2V Fixed at 25 m				P2V Optimized				
		V(#)	V/S(%)	μ (m)	σ (m)	V(#)	V/S(%)	μ (m)	σ (m)	thresh(m)
D V	1	329	74.8	40.0	26.1	319	81.2	39.4	26.4	35
	2	210	96.8	22.5	14.3	147	99.3	20.9	12.3	63
	3	-	-	-	-	-	-	-	-	-
	8	198	56.3	54.1	18.3	159	74.3	53.1	18.0	35
N T S	4	229	97.9	17.0	8.4	324	99.1	18.1	10.3	12
	5	246	100	12.5	6.4	307	99.0	14.2	10.0	12
	6	236	81.9	58.1	18.3	52	96.3	53.6	16.3	75
	7	106	99.1	11.0	7.5	134	99.3	12.3	10.3	14

ground truth had noticeable biases in some flights.

The analysis included two ways of labeling estimates as “sure” by applying two different sets of thresholds on the confidence metrics. The first way labeled all position estimates in all flights with P2V greater than 25 m as sure. This threshold was picked to work well in all flights; nonetheless it is specific to the terrain relief in this field test. The second way consecutively applied thresholds on two metrics. First, position estimates with very large correlation width were dismissed as unsure. Then, the P2V threshold was adjusted for each flight such that 99% (or as much as possible) of the estimates above the threshold had errors less than 90 m. This meant that TRN would allow for only 1% incorrect estimates to be passed on to navigation. The first way, dubbed fixed threshold method, was useful for comparing results across flights, while the second way, dubbed optimized threshold method, showed the effect of minimizing the number of incorrect estimates passed on to navigation for each flight. Table 1 summarizes the performance metrics for these methods. Results for flight 3, which had some problems with the trajectory, were not shown.

A. Fixed Threshold Method

To assess the performance of the LIDAR TRN algorithm, the horizontal position errors were plotted versus the P2V confidence metric. As seen in Fig. 2, the position estimates for flights 2, 4, 5, and 7 were very good. Their error clustered near zero and was typically less than 50 m. The P2V confidence metric set apart mostly correct estimates above its threshold.

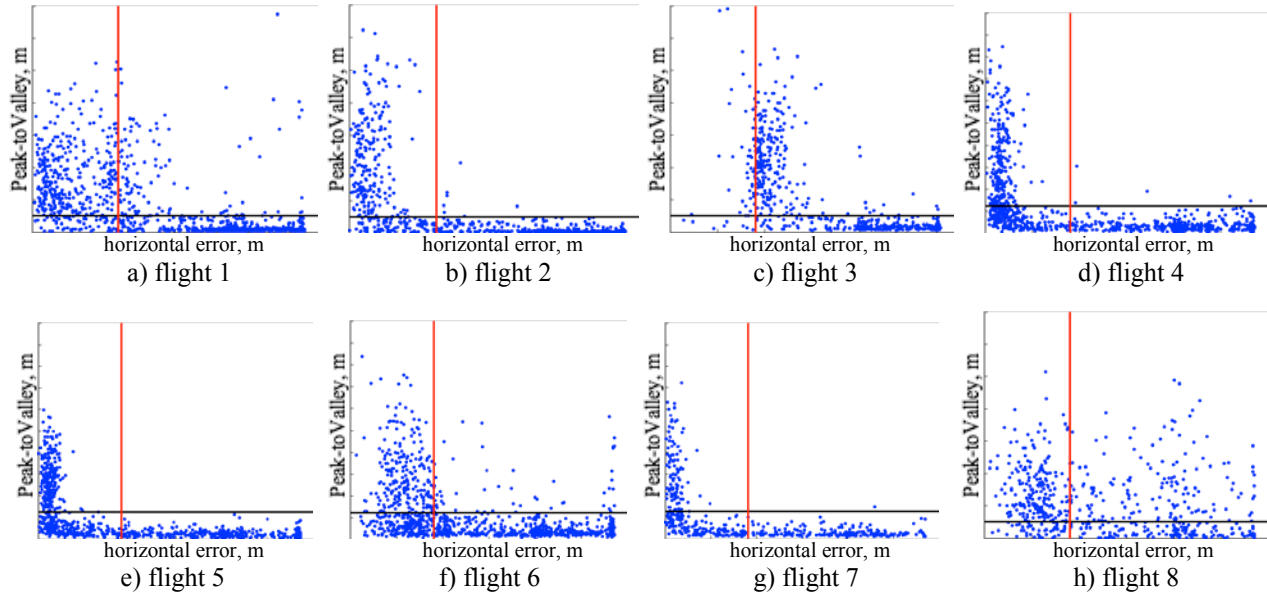


Figure 2. TRN performance for all flights. These plots show the distribution of error for the TRN position estimates (blue dots) across flights and the confidence established by the fixed P2V threshold of 25 m (black line). For most flights, the estimates above this threshold are below the 90 m requirement (red line).

The position error of flights 1, 3, 6, and 8 had a wide variation. Notice, that in flights 3, 6, and 8 the cluster of position errors had moved away from zero. This fact suggests an unknown and constant misalignment, which caused problems with the ground truth trajectory. This misalignment might have been caused during the relocation of some sensors on the airplane. Additionally, during flight 8, the LIDAR had problems outputting its clock rate, making it impossible to calibrate the range and make accurate LIDAR maps. Moreover, the 5x divergence was used on the flash LIDAR laser in flights 1, 3, 6, and 8, which resulted in about 100 triggering pixels per image when the plane was at 2 km altitude and 50 or fewer at higher altitude. In flights 2, 4, 5, and 7 the 2x divergence was used, which resulted in 400 pixels at 2 km and 200 pixels at 4 km altitude. This difference meant that the LIDAR contours for flights 1, 3, 6, and 8 were narrower than those of the other flights; thus the larger spread in error.

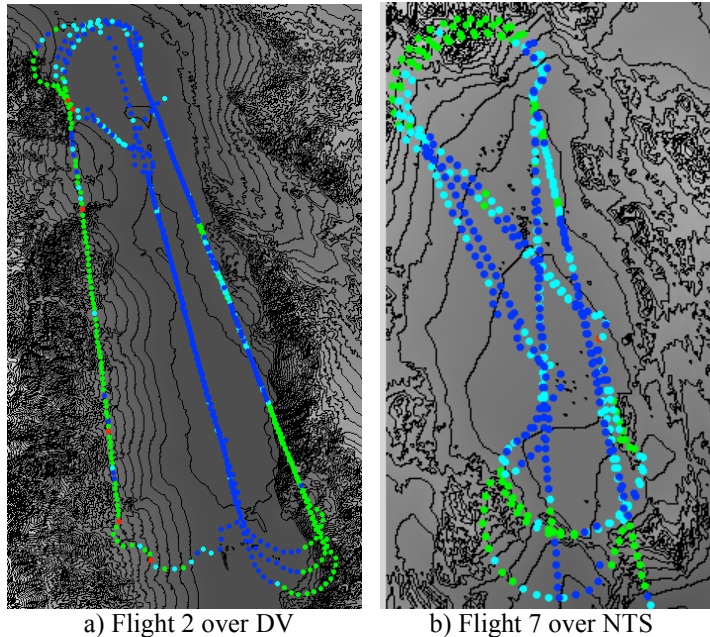


Figure 3. Position estimation results for the fixed threshold method. Legend: correct and sure in green, incorrect but sure in red, correct but unsure in cyan, and incorrect and unsure in blue

The position estimation results for flights 2 and 7 were plotted on a contour map of the corresponding test site in Fig. 3. The results were colored according to their category. It is seen that most errors occurred in the flat portions of the terrain, whereas most correct estimates were over the rougher terrain. Therefore, the performance of LIDAR TRN is driven by the amount of terrain relief present in the LIDAR data.

B. Optimized Threshold Method

Flights 1, 3, 8, and 6 had some issues as described above. The optimized threshold method succeeded in flights 2, 4, 5, and 7, which were highlighted in green in Table 1. For these flights, the average valid mean error μ was 15.8 m for the fixed and 16.4 m for the optimized method. The average valid standard deviation σ was 9.2 m for fixed and 10.7 m for the optimized method. The average valid over sure fraction was 98.5% for fixed and 99.2% for optimized method. This meant that in 100 estimates TRN would allow only 1 incorrect, which can certainly be taken care of by the Kalman filter inside navigation.

The estimates that were dismissed as unsure due to extremely wide peak were mostly ones with high error and low P2V. Thus, this metric was mostly subsumed by P2V. When P2V indicated that the terrain had sufficient features, LIDAR TRN gave us position estimates well inside the 90 m requirement with very high confidence.

The aim of the optimized threshold method was to have the highest number of valid estimates, while maintaining a very low number of incorrect and sure estimates. For flights 4, 5, and 7 the optimized threshold was lower than the fixed one and a greater number of valid estimates were obtained. However, there was a trade off – the valid mean error and standard deviation increased. Thus, for gaining more valid estimates, their average error was larger but still within requirement. In flights 2, 6, and 8, where there were many incorrect estimates with high P2V, the optimized threshold was raised above the fixed and a significant number of valid estimates were thrown out in order to achieve the highest possible confidence. Here, we traded off was higher confidence in valid estimates for lesser number of valid estimates.

VI. Sensitivity Studies

In addition to processing the LIDAR data from all flights, studies were conducted to assess the sensitivity to confidence metric, contour length, map resolution, and initial position uncertainty. Because of its relatively good performance, flight 2 was used in these studies.

A. Confidence Metric Study

After observing plots, such as those in Fig. 2, for all confidence metrics, it was found out that P2V and TRI were the best metrics. Almost all estimates above their respective thresholds (25 m for P2V and 1 m for TRI) were valid. Both of these metrics describe terrain relief and utilize the fact that higher relief results in better TRN estimates.

The contour size and shape did not have an observable relation with the error. This confirmed the intuition that it was only necessary to have one unique feature in the contour to lock in the correlation. Also, if the contour had no features and was flat, its shape did not improve error.

The correlation peak height, peak width, and peak ratio were able to throw out estimates with high error, which occurred because of very flat terrain that was hard to match. However, these metrics were mostly subsumed by the P2V and the TRI metrics.

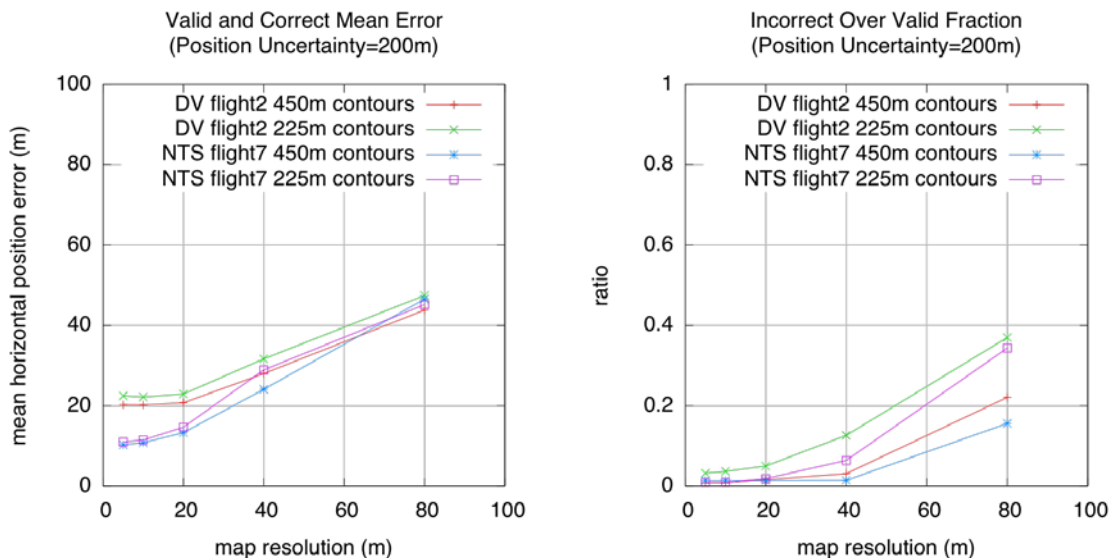


Figure 4. Map resolution sensitivity study. These plots show the estimates as a function of map resolution for flights 2 and 7.

B. Contour Length Study

This study aimed to determine the contour length that generated the highest total number of valid estimates as predicted by the confidence metrics. Five sets of contours were generated with different lengths using: 600, 300, 150, 75, and 37 images. Note that 600 images represent 60 s of data and about 3600 m of flight path. Although all contours in each set used the same number of images, they had different size and shape depending on the gimbal mode.

As the segment size got shorter, the TRN updates became more frequent; thus, the total number of estimates increased. It was observed that the total number of valid estimates detected by the metrics also increased, giving a higher rate of confident estimates passed on to navigation. However, the marginal increase became smaller every time the length was cut in half. Also, the error of the valid estimates increased by a few meters. Furthermore, confident but incorrect estimates started appearing. Therefore, the number of valid estimates increased, but the quality of these estimates degraded with shorter segment length. For the terrains in this test, the contour length that maximized the number of valid estimates while keeping the confident and incorrect estimates to a minimum was 75 images.

C. Map Resolution Study

The LIDAR TRN algorithm is based on correlation between a LIDAR DEM and a reference DEM. The greater the resolution of the maps, the less accurate is the peak fitting procedure done during correlation and, consequently, the less accurate are the position estimates. To assess the sensitivity to map resolution, flight 2 and 7 were used.

As seen in the left plot of Fig. 4, the mean error of the position estimates increased as the map resolution increased. There was a linear growth in the mean error when resolution was between 20 and 80 m. However, there was essentially no change in error when resolution was between 5 and 20 m. This discrepancy was likely due to an error in the ground truth on the order of 20 m, which caused the constant estimate error despite change in resolution. Also, flight 2 over DV initially had twice as much error as flight 7 over NTS. This was probably due to the ground truth error being larger for DV than NTS.

As seen in the right plot of Fig. 4, the incorrect over sure fraction increased as the map resolution increased. The terrain relief was being smoothed as map resolution increased. With less terrain relief, the contours became less unique, which increased the chance of incorrect matches.

D. Position Uncertainty Study

Plots of the performance metrics as a function of the position uncertainty for flights 2 and 7 are shown in Fig. 5. The valid mean error and the incorrect over sure fraction did not change with uncertainty. Therefore, the LIDAR TRN algorithm is not sensitive to the position uncertainty and could easily handle the initial position uncertainties of about 1 km expected during lunar landing. However, as the position uncertainty increased, the size of the correlation search area increased, and so did the computation time of the algorithm.

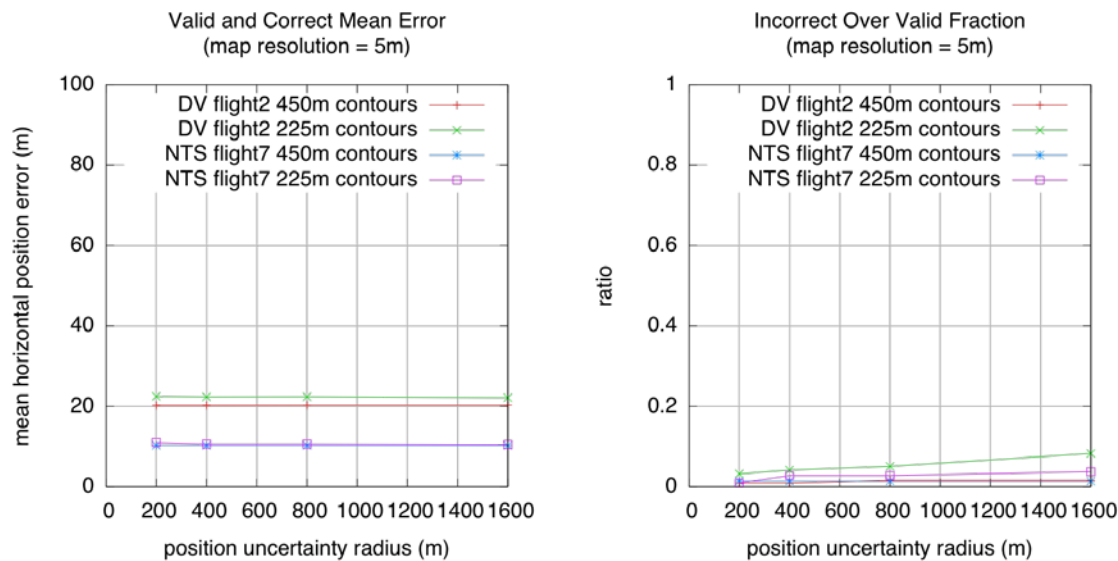


Figure 5. Position uncertainty sensitivity study. These plots show the estimates as a function of position uncertainty for flights 2 and 7.

VII. Conclusion

The TRN approach presented here, based on correlation of LIDAR data and elevation map, meets the objective of 90 m landing precision under any lighting conditions. TRN estimates have error typically less than 50 m. Most incorrect estimates are eliminated using confidence metrics based on terrain relief. Instrument misalignments are the main causes of large global errors. Disregarding those, 99% of the TRN estimates passed on to the navigation filter are accurate. Also, the algorithm can handle initial uncertainty of 1.6 km without performance degradation. Nevertheless, TRN performance degrades with larger map resolutions.

Future work will include a study of the effect of contour width on TRN performance. Also, pre-filtering of the contours through a band-pass filter or masking out flat regions will be investigated to sharpen the correlation peak. Using laser altimeter data with the LIDAR TRN algorithm will also be investigated.

Acknowledgments

The work described in this publication was performed at the Jet Propulsion Laboratory, California Institute of Technology, under contract from the National Aeronautics and Space Administration.

References

- ¹Johnson, A., and Montgomery, J., "Overview of Terrain Relative Navigation Approaches for Precise Lunar Landing," *Proc. of the IEEE Aerospace Conference*, Big Sky, MT, 2008.
- ²Aggarwal, J., and Sabata, B., "Estimation of Motion from a Pair of Range Images: A Review," *Computer Vision, Graphics, and Image Processing*, Vol. 54, No. 3, 1991, pp. 309-324.
- ³Shah, M. and Kumar, R., (eds.), *Video Registration*, Kluwer Academic Publishers, Boston, 2003, Chapter 7 "Geodetic Alignment of Aerial Video Frames," by Sheikh, Y., Khan, S., Shah, M., and Cannata, R.
- ⁴Gaskell, R., "Automated Landmark Identification for Spacecraft Navigation," *Proc. of the AAS/AIAA Astrodynamics Specialists Conference*, 2001.
- ⁵Cheng, Y., and Ansar, A., "Landmark Based Position Estimation for Pinpoint Landing on Mars," *Proc. of the IEEE Int'l Conf. on Robotics and Automation (ICRA)*, Barcelona, Spain, 2005, pp. 4470-4475.
- ⁶Johnson, A. et al., "A General Approach to Terrain Relative Navigation for Planetary Landing," *Proc. the AIAA Infotech at the Aerospace Conference*, Rohnert Park, CA, 2007.
- ⁷Epp, C. and Smith, T., "The Autonomous Precision Landing and Hazard Detection and Avoidance Technology (ALHAT)," *Proc. of the Aerospace Conference*, Big Sky, MT, March 2008, pp. 1-7.
- ⁸Golden, J. P., "Terrain Contour Matching (TERCOM): a Cruise Missile Guidance Aid," *Image Processing for Missile Guidance, Proc. of the Society of Photo-optical Instrumentation Engineers*, Vol. 238, 1980, pp. 10-18.
- ⁹Carr, J. C., and Sobek, J. L., "Digital Scene Matching Area Correlator (DSMAC)," *Image Processing for Missile Guidance, Proc. of the Society of Photo-Optical Instrumentation Engineers*, Vol. 238, 1980, pp. 36-41.
- ¹⁰Johnson, A., and SanMartin, M., "Motion Estimation from Laser Ranging for Autonomous Comet Landing," *Proc. of the Int'l Conf. on Robotics and Automation (ICRA)*, San Francisco, CA, 2000, pp. 132-138.
- ¹¹Riley, S., DeGloria, S., and Elliot, R., "A Terrain Ruggedness Index That Quantifies Topographic Heterogeneity," *International Journal of Science*, Vol. 5, No. 1-4, 1999, pp. 23-26.
- ¹²Keim, J., "Field Test Implementation to Evaluate a Flash Lidar as a Primary Sensor for Safe Lunar Landing," *Proc. of the Aerospace Conference*, Big Sky, MT, March 2010, paper 2.0304.